THE JOURNAL OF BIOLOGICAL CHEMISTRY VOL. 287, NO. 26, pp. 21980–21991, June 22, 2012

Okazaki Fragment Processing-independent Role for Human Dna2 Enzyme during DNA Replication*[S]

Received for publication, March 5, 2012, and in revised form, April 25, 2012 Published, JBC Papers in Press, May 7, 2012, DOI 10.1074/jbc.M112.359018

Julien P. Duxin[‡§], Hayley R. Moore[‡§], Julia Sidorova[¶], Kenneth Karanja[‖], Yuchi Honaker[‡§], Benjamin Dao[‡§], Helen Piwnica-Worms[‡§], Judith L. Campbell[‖], Raymond J. Monnat, Jr.[¶], and Sheila A. Stewart[‡§**1]**

*From the [‡]Department of Cell Biology and Physiology, [§]BRIGHT Institute, St. Louis, Missouri 633110, the [¶]Department of Pathology, University of Washington, Seattle, Washington 98195, [‖]Braun Laboratories, California Institute of Technology, Pasadena, California 91125, and the **Department of Medicine, Washington University School of Medicine, St. Louis, Missouri 633110*

Background: Dna2 and FEN1 putatively cooperate in Okazaki fragment (OF) processing in yeast.
Results: FEN1 depletion leads to OF maturation defects that do not impact replication fork kinetics, whereas hDna2 depletion leads to DNA damage independent of OF maturation.
Conclusion: hDna2 participates in DNA replication in a manner distinct from FEN1.
Significance: hDna2 participates in replication in a FEN1, OF maturation-independent manner.

Dna2 is an essential helicase/nuclease that is postulated to cleave long DNA flaps that escape FEN1 activity during Okazaki fragment (OF) maturation in yeast. We previously demonstrated that the human Dna2 orthologue (hDna2) localizes to the nucleus and contributes to genomic stability. Here we investigated the role hDna2 plays in DNA replication. We show that Dna2 associates with the replisome protein And-1 in a cell cycle-dependent manner. Depletion of hDna2 resulted in S/G_2 phase-specific DNA damage as evidenced by increased γ-H2AX, replication protein A foci, and Chk1 kinase phosphorylation, a readout for activation of the ATR-mediated S phase checkpoint. In addition, we observed reduced origin firing in hDna2-depleted cells consistent with Chk1 activation. We next examined the impact of hDna2 on OF maturation and replication fork progression in human cells. As expected, FEN1 depletion led to a significant reduction in OF maturation. Strikingly, the reduction in OF maturation had no impact on replication fork progression, indicating that fork movement is not tightly coupled to lagging strand maturation. Analysis of hDna2-depleted cells failed to reveal a defect in OF maturation or replication fork progression. Prior work in yeast demonstrated that ectopic expression of FEN1 rescues Dna2 defects. In contrast, we found that FEN1 expression in hDna2-depleted cells failed to rescue genomic instability. These findings suggest that the genomic instability observed in hDna2-depleted cells does not arise from defective OF maturation and that hDna2 plays a role in DNA replication that is distinct from FEN1 and OF maturation.

Genomic maintenance requires coordination of several processes including DNA replication, DNA repair, transcription, and cell cycle progression. Given the importance of genomic stability for ongoing cell proliferation, it is not surprising that DNA replication and repair proteins have evolved multiple functions and participate in several replication and repair pathways. Previously, we demonstrated that human Dna2 (hDna2)[2] localizes to the nucleus and mitochondria and participates in DNA maintenance in both compartments (1). Dna2 is a highly conserved helicase/nuclease, originally discovered in *Saccharomyces cerevisiae* and found in all organisms from yeast to humans (2–6). Dna2 possesses a 5′ to 3′ ATP-dependent helicase activity and a flap endonuclease activity (7). Genetic and biochemical experiments conducted in yeast support a model in which Dna2 contributes to Okazaki fragment (OF) maturation in lagging strand DNA replication (8–10), although *in vivo* evidence of Dna2 participating in this process is lacking.

During OF processing, flap endonuclease 1 (FEN1) is the major endonuclease that acts in a coordinated manner with DNA polymerase δ strand displacement activity to remove short RNA/DNA flaps formed on the previous OF (short flap pathway OF processing) (9–12). Flaps that escape FEN1 cleavage and are longer than 27 nucleotides are subsequently coated by replication protein A (RPA), which inhibits FEN1 nuclease activity (long flap pathway OF processing) (9, 12, 13). RPA-bound OF flaps recruit Dna2, which cleaves the RPA-coated DNA and displaces RPA, leaving a short 5–6-nucleotide RNA-free DNA flap that is further processed by FEN1 to produce a ligatable nick (9, 10, 14–18). In support of this long flap model, both PIF1 helicase and polymerase δ processivity subunit (Pol 32) promote long flap formation *in vitro*, and their deletion rescues the lethality associated with yeast Dna2 loss, presumably because long flaps no longer form (12, 19–22). Conversely, mutations that increase polymerase δ processivity are synthetically lethal with *dna2* mutations (19).

* This work was supported, in whole or in part, by National Institutes of Health Grants GM95924 (to S. A. S.), GM04701 and GM04707 (to H. P.-W.), P01 CA77852 (to R. J. M.), and GM078666 (to J. L. C.). This work was also supported by the Department of Defense Grant CDMRP 09-0-0041, Cancer Biology Pathway, Siteman Cancer Center at Barnes-Jewish Hospital, and Washington University School of Medicine in St Louis (to J. P. D. and H. R. M.).
[S] This article contains supplemental Figs. 1–3.
[1] To whom correspondence should be addressed: Dept. of Cell Biology and Physiology, Washington University School of Medicine, 660 South Euclid Ave., Campus Box 8228, St. Louis, MO 63110. Tel.: 314-362-7437; Fax: 314-362-7463; E-mail: sheila.stewart@wustl.edu.

[2] The abbreviations used are: hDna2, human Dna2; OF, Okazaki fragment; FEN1, flap endonuclease 1; RPA, replication protein A; DSB, double strand breaks; ICB, internuclei bridges; maRTA, microfluidic-assisted replication track analysis; LigI, ligase I.

In addition to its role in OF processing, Dna2 functions in DNA repair and telomere maintenance through its DNA end-resection activity. In yeast, Dna2 undergoes a dynamic localization where it is present at telomeres in G_1, relocalizes throughout the genome in S phase, and moves back to the telomeres in late S/G_2 phase (23). In addition, upon bleomycin treatment, yeast Dna2 leaves the telomere and localizes to sites of double strand breaks (DSBs) (23). Recent studies have demonstrated that yeast Dna2 nuclease activity participates in the formation of a 3′ single strand DNA overhang essential to initiate the homologous recombination process or to maintain telomeric stability (24–30). Furthermore, Nimonkar *et al.* (31) elegantly reconstituted DNA end resection *in vitro* using purified human proteins and demonstrated that hDna2 physically interacts with Bloom to resect 5′ DNA ends in a process that depends on hDna2 nuclease but not hDna2 helicase activity. Nonetheless, *in vivo* and *in vitro* studies in yeast and humans indicate that Exo1 can compensate for Dna2 nuclease activity in this process (24, 29, 31). This suggests that the essential function of Dna2 is not its resection activity during DSB repair but rather its function in removing long flaps during DNA replication.

Our previous work revealed that hDna2 contributes to genomic stability (1). Here, we provide evidence that hDna2 ensures genomic stability by virtue of a critical role in DNA replication that is independent of FEN1 and OF processing.

EXPERIMENTAL PROCEDURES

Cell Culture—U-2-OS and HeLa were grown in Dulbecco's modified Eagle's medium (DMEM) (Sigma) containing 10% heat-inactivated fetal bovine serum (FBS) and 1% penicillin/streptomycin at 37 °C in 5% CO_2.

Virus Production and Infection—Viral production and infections were carried out as described previously (1, 32). Briefly, 293T cells were transfected using TransIT-LT1 (Mirus, Madison, WI), and virus was collected 48 h post-transfection. Subsequent infections were carried out overnight in the presence of 10 μg/ml protamine sulfate and followed 48 h post-infection by selection of transduced cells with 2 μg/ml of puromycin. The pLKO.1 shDna2, pResQ shDna2′, and pLKO.1 shSCR lentiviruses were produced by co-transfection with pCMV8.2ΔR and pCMV-VSV-G (8:1 ratio). The sequence for the shDna2 short hairpin was 5′-CATAGCCAGTAGTATTCGATG-3′, for shDna2′ was 5′-GCAGTATCTCCTCTAGCTAGT-3′, and for shSCR was 5′-AAGGTTAAGTCGCCCTCGCTC-3′ as previously reported (1). The sequences used for the FEN1 short hairpins were previously reported (32). The sequence used for the LigI-specific shLigI was 5′-GCTCAAGCTGAAGAAGGACTA-3′.

The pBabe-hygro-3xFLAG-Dna2 wild-type (wt), D294A (nuc), K671E (hel), and D294A/K671E double mutant (dm) cDNAs were cloned from pFastBACHTc-hDna2-FLAG and confirmed by DNA sequencing (5). Briefly, depletion rescue experiments utilized pBabe-Hygro-3XFLAG-Dna2 (wt, nuc, hel or dm) or pBabe-hygro-3×FLAG control constructs produced in 293T cells. U-2-OS cells were transduced with different constructs and selected in the presence of 200 μg/ml hygromycin B (Sigma). After selection, hDna2 overexpression was confirmed by Western blot, and cells were transduced with pResQ shDna2′, which does not target the exogenous hDna2 cDNAs followed by puromycin selection as described above. Five days post-infection, cells were analyzed for DNA content by flow cytometry as previously described (Fig. 2*A*) (1).

For FEN1 ectopic expression experiments, viral production and infections were carried out as described previously (32). U-2-OS cells were infected with pLKO.1 shSCR or pLKO.1 shDna2 lentiviruses for 5 h. Cells were then counted and reseeded in the presence of media containing Adeno-FEN1 or Adeno-GFP (33). 48 h post-infection cells were re-plated at 0.8×10^6 cells/10-cm plate and then analyzed 24 to 48 h later by hypotonic propidium iodide staining and flow cytometry as previously described (1). FEN1 ectopic expression was confirmed by Western blot and immunofluorescence (data not shown).

Immunoprecipitation and Western Blot Analysis—For co-immunoprecipitation studies, cells were washed in PBS and lysed in TBS-Triton X-100 buffer containing 50 mM Tris-HCl, pH 7.4, 150 mM NaCl, 1 mM EDTA, 1% Triton X-100, and protease and phosphatase inhibitors. 2 mg of protein extracts were immunoprecipitated with 2.4 μg of anti-hDna2 or IgG control antibodies using protein A beads overnight at 4 °C. The following morning beads were washed 3 times in 1 ml of TBS-Triton X-100 buffer before eluting bound proteins in 2× Laemmli buffer by boiling for 5 min at 95 °C. Anti-hDna2 antibody was produced as previously described (5), and anti-And-1 was kindly provided by Dr. Anindya Dutta (34).

For the cell cycle experiments, cells were enriched in G_0/G_1 and G_1/S by serum starvation and double thymidine block, respectively, as previously described (35). Briefly, for G_0/G_1 enrichment, exponentially growing cells were cultured in DMEM medium containing 0.6% FBS for 38 h, then harvested, analyzed by FACS to ensure arrest, and used for immunoprecipitation of hDna2 followed by Western blotting for And-1. For G_1/S enrichment, exponentially growing cells were cultured in medium supplemented with 3 mM thymidine for 16 h and washed twice in pre-warmed PBS, and fresh medium without thymidine was added for 12 h. Then, fresh medium with 3 mM thymidine was added, and cells were grown for another 16 h. Arrest was monitored by flow cytometry analysis, and cells were harvested and used for co-immunoprecipitation studies as described above.

For Western blot analysis, cells were washed in phosphate buffered saline (PBS), lysed in MCL buffer (50 mM Tris, pH 8.0, 5 mM EDTA, 0.5% Nonidet P-40, 100 mM NaCl, 2 mM DTT, and freshly added protease and phosphatase inhibitors), sonicated (6 cycles of a 30-s pulse and 30-s cooling interval), and centrifuged for 20 min at 4 °C. Western blot analysis was carried out on whole cell lysates with the following antibodies: anti-hDna2 (ab96488, Abcam, Cambridge, MA); anti-FEN1 (A300–255A, Bethyl Laboratories, Montgomery, TX); anti-DNA Ligase I (ab615, Abcam, Cambridge, MA); anti-FLAG M2 (F3165, Sigma); anti-Chk1 (G-4 #SC-8408, Santa Cruz, Santa Cruz, CA); anti-phospho-Chk1 (Ser-317) (36) (Cell Signaling); anti-β-catenin (#610154, BD Biosciences); anti-γ-actin (NB600-533, Novus Biological, Littleton, CO); anti-phospho-histone H3 (Ser-10) (#9701, Cell Signaling). For Western blot analysis of γ-H2AX, cells were washed with PBS and lysed in radioimmune

precipitation assay buffer (150 mM NaCl, 1% Triton X-100, 0.5% sodium deoxycholate, 0.1% SDS, 50 mM Tris, pH 8.0, and freshly added protease and phosphatase inhibitors) then probed with anti-phospho-histone H2A.X (Ser-139) (clone JBW301, #05-636, Millipore, Temecula, CA). All protein concentrations were measured using the Bradford assay.

Immunofluorescence—U-2-OS cells were grown for 1–2 days on coverslips, then washed in PBS, fixed in 4% paraformaldehyde, and permeabilized in 0.5% Triton X-100 before treatment with blocking buffer (10% FBS, 2% goat serum, and 0.2% Tween 20) at room temperature. Antibodies were diluted in blocking buffer and incubated with cells for 1 h at room temperature or overnight at 4 °C. Cells were washed in PBS containing 0.02% Tween 20 and mounted in ProLong Gold mounting medium (Invitrogen) containing 4′, 6-diamidino-2-phenylindole (DAPI). Immunofluorescence detection was carried out with anti-phospho-histone H2A.X (Ser-139) (clone JBW301, #05-636, Millipore) or anti-phospho-ATM (Ser-1981) (clone 10H11.E12, #4526, Cell Signaling) as primary antibodies. Secondary antibodies were anti-mouse IgG-Alexa-Fluor® 488 or 546 (Invitrogen).

For RPA immunofluorescence, cells were pre-extracted before fixing as previously described (37). Briefly, U-2-OS cells were grown for 1–2 days on coverslips. Cells were washed in ice-cold cytoskeleton (CSK) buffer (10 mM HEPES/KOH, pH 7.4, 300 mM sucrose, 100 mM NaCl, 3 mM $MgCl_2$) and then extracted for 6 min on ice with 0.5% Triton X-100 in CSK buffer supplemented with protease and phosphatase inhibitors. After extraction, cells were fixed in 3.7% formaldehyde at room temperature for 25 min followed by immunofluorescence staining using anti-replication protein A antibody (RPA-70-9, #NA13, Calbiochem).

Internuclei Chromatin Bridges and Micronuclei Counts—hDna2-depleted (shDna2 and shDna2′) and control (shSCR) U-2-OS cells were seeded in a 12-well plate at 5×10^4 cells per well 4 days post-infection. After 36–48 h, cells were fixed and stained with DAPI, and the number of internuclei bridges (ICBs) and micronuclei were counted. At least 1000 nuclei were counted per well, and 6 wells were quantified per experiment. Two independent experiments were quantified for micronuclei counts in Fig. 1*C* and ICB counts in Fig. 5*D*. To inhibit Chk1, cells were treated with either 300 nM Gö 6976 (Calbiochem) (38) or 100 nM AZD7762 (Axon Medchem BV, The Netherlands) (39) for 8 h before fixing and quantification of ICBs. Inhibition of Chk1 was confirmed by flow cytometry and Western blot (Fig. 5*C* and data not shown). Images were processed using Photoshop 7.0 gray scale and invert function (Adobe, San Jose, CA).

Flow Cytometric Analysis—U-2-OS cells were seeded at 0.8×10^6 cells/10-cm plate 4 days post-infection and resuspended 36–48 h later for hypotonic propidium iodide staining (0.1% sodium citrate tribasic, 0.3%Triton X-100, 0.01% propidium iodide, 50 μg/ml RNase A (Sigma)) before flow cytometry to determine DNA content as previously described (40).

S Phase Progression Assay—U-2-OS cells were cultured for 30 min in the presence of 20 μM bromo-2-deoxyuridine (BrdU) in the dark as previously described (33). Briefly, cells were washed, cultured in fresh medium, and harvested by trypsinization at the indicated times. Cells were washed in PBS and fixed in 4% paraformaldehyde and 0.1% Triton X-100 in PBS for 20 min at room temperature before DNase I treatment (30 μg DNase I (Sigma) at 37 °C for 1 h). BrdU was detected with an Alexa Fluor 488-conjugated anti-BrdU antibody (A21303, Invitrogen), and cellular DNA content was determined by propidium iodide staining followed by flow cytometric analysis.

Metaphase Preparation and Chromosome FISH—Subconfluent U-2-OS cells were incubated for 3.5–4 h with 0.1 μg/ml colcemid to isolate mitotic cells by mitotic shake-off. After hypotonic swelling in 75 mM KCl for 10 min at 37 °C, cells were fixed in methanol/acetic acid (3:1), dropped onto glass slides, and aged at room temperature for 3 days. FISH was performed as previously described (32). Briefly, slides were rehydrated for 10 min in PBS, fixed with 4% paraformaldehyde in PBS for 2 min, then hybridized with 0.3 μg/ml telomeric PNA probe (Cy3-$(CCCTAA)_3$) and a centromeric probe (Flu-OO-CTT-CGTTGGAAACGGGA) in 70% formamide, 10 mM Tris HCl, pH 7.2, plus blocking reagent (Roche Applied Science). DNA was denatured for 3 min at 80 °C, and hybridizations were carried out at 37 °C for 4 h in a moist chamber. Slides were subsequently washed, dehydrated, and mounted using VectaShield (Vector Labs, Burlingame, CA) containing DAPI. Images were taken using a Nikon 90i microscope and analyzed using the ISIS FISH imaging software (Metasystems, Altlussheim, Germany).

BrdU-comet Assay—The BrdU-comet assay was performed as previously described (41). Briefly, U-2-OS cells were plated at 5×10^5 cells/6-cm plate and grown for 36 h at 37 °C. Cells were then pulsed for 30 min with 100 μM BrdU (Sigma) and chased for 1–8 h in growth medium lacking BrdU. Cells were then trypsinized and embedded in low melting point agarose at 37 °C before spreading onto comet slides (Trevigen, Gaithersburg, MD). Cells on slides were then lysed, denatured, and run through electrophoresis under denaturing conditions (200 mM NaOH, 1 mM EDTA) before immunostaining with anti-BrdU antibody (#555627, BD Biosciences) for 1 h in the dark. The primary antibody was detected using anti-mouse IgG-Alexa-Fluor® 488 (Invitrogen), and cells were counterstained with DAPI. At least 40 comet tails were quantified per sample time point using CometScore™ (TriTek). A total of three independent experiments were conducted.

Microfluidic-assisted Replication Track Analysis (maRTA) Assay—Replication fork progression rates were determined using maRTA (42). Briefly, hDna2-depleted (shDna2) or control (shSCR) U-2-OS cells were labeled for 30 min each with 50 μM IdU followed by 50 μM CldU (Sigma). For FEN1-depleted cells, U-2 OS-hTert cells were used to avoid potential telomeric defects induced by FEN1 depletion (43). Cells were then collected by trypsinization and used to prepare agarose plugs as previously described (42). High molecular weight DNA was isolated from cells embedded in agarose by brief heating to 75 °C to melt the agarose followed by agarose digestion. The resulting high molecular weight DNA was then loaded by capillary tension into microchannels to uniformly stretch and capture long, high molecular weight DNA molecules on glass coverslips for immunostaining and fluorescence microscopy. Origin firing efficiency was determined by counting the fraction of origin

firing events among all active replication events. Replication elongation efficiency was determined by measuring the mean length of first-label replication tracks in double-labeled tracks to analyze active/ongoing fork rates. Track lengths were measured in digital images of track using the AxioVision software package (Carl Zeiss). Three replicate samples of hDna2-depleted U-2-OS cells or mock-depleted U-2-OS cells (hDna2 experiment) or FEN1 depleted U-2 OS-hTert *versus* mock-depleted U-2 OS-hTert cells (FEN1 experiment) were analyzed for each determination. A total of 250–450 replication tracks were measured in each sample.

RESULTS

hDna2 Contributes to Genomic Stability—We previously reported that hDna2 depletion in U-2-OS cells leads to genomic instability characterized by the appearance of aneuploid cells, ICBs, and an accumulation of cells in the late S/G_2 phase of the cell cycle (1). Here we further report that hDna2 depletion results in an increase in γ-H2AX, a well characterized marker of DNA damage including DSBs, and the appearance of micronuclei indicative of aberrant mitosis. U-2-OS cells were transduced with one of two shRNA hairpins that led to a greater than 70% reduction in hDna2 mRNA and protein levels (Fig. 1, *A* and *B*). Analysis of hDna2-depleted cells revealed a 2-fold increase in micronuclei compared with cells expressing a control shRNA (Fig. 1*C*). Furthermore, hDna2-depleted cells displayed an increase in γ-H2AX foci that was confirmed by Western blot analysis (Fig. 1, *B* and *D*). In addition to the appearance of γ-H2AX foci, we also observed phosphorylated-ATM foci in hDna2-depleted cells (Fig. 1*D*), confirming that hDna2 depletion results in the generation of DNA damage with activation of the DNA damage checkpoint.

ICBs arise from unresolved replication intermediates, defective mitosis, and/or telomere fusions that form upon loss of telomeric integrity (44). Because Dna2 plays an important role in telomere stability in yeast, we investigated whether the ICBs observed upon hDna2 depletion were the result of telomeric fusions. To address this possibility, we analyzed metaphases from control or hDna2-depleted cells. No increase in chromosomal end-to-end fusions was observed in cells expressing shRNAs targeting hDna2, suggesting that telomere dysfunction is not responsible for the formation of ICBs in these cells (supplemental Fig. 1). Interestingly, analysis of metaphases isolated from hDna2-depleted cells revealed the appearance of abnormal chromosomes (Fig. 1*E*). These metaphases are reminiscent of chromosomes isolated from cells entering mitosis with incompletely replicated DNA (45) that could lead to the generation of ICBs, DSBs, and micronuclei similar to what is observed in hDna2-depleted cells. Together these experiments suggest that the genomic instability observed in hDna2-depleted cells arises from incomplete DNA replication.

hDna2 Nuclease and Helicase Activities Are Essential—Dna2 is a highly conserved enzyme that possesses nuclease and helicase/ATPase activities that are postulated to contribute to its function *in vivo*. Although both activities are essential for viability in *S. cerevisiae* (46), recent *in vitro* biochemical studies have called into question the significance of the helicase activity in the human protein (5, 6). Therefore, we addressed whether

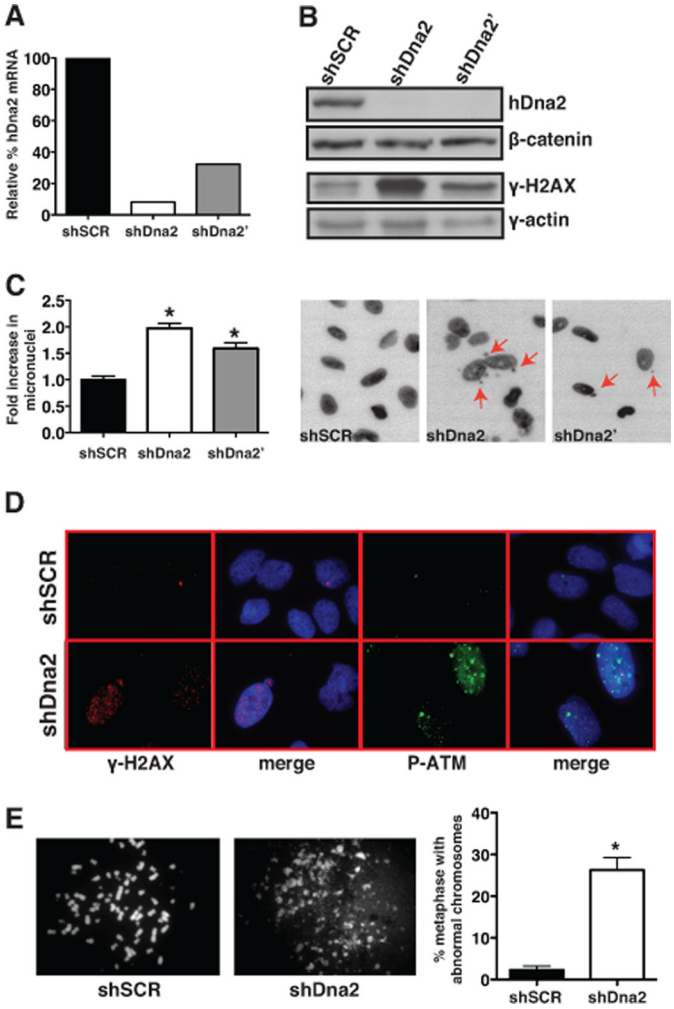

FIGURE 1. **hDna2 contributes to genomic maintenance.** *A*, knockdown of hDna2 in U-2-OS cells was determined by quantitative RT-PCR. Results for two independent hairpins targeting hDna2 (*shDna2* and *hDna2′*) are normalized to the shSCR control cell line expression levels. Note: shDna2 induces a better knockdown of hDna2 mRNA than shDna2′. *B*, hDna2 knockdown was determined by Western blot analysis. Lysates were also probed for γ-H2AX to assess DNA damage and DSBs. *C*, shown are relative micronuclei counts and representative images depicting micronuclei (*red arrows*) after hDna2 depletion in cells. Results were normalized to shSCR control cells. *D*, shown is immunofluorescence staining of γ-H2AX (*red*) and phosphorylated-ATM (*P-ATM*) (*green*) in U-2-OS cells depleted of hDna2 (*shDna2*, *bottom panels*) or a control hairpin (*shSCR*, *top panels*). Nuclei were stained with DAPI (*blue*). *E*, *left*, shown is metaphase spread of control cells and hDna2-depleted cells with abnormal chromosomes. *Right*, quantification of 200 metaphases from 2 independent experiments is shown. All *error bars* represent S.E., and * denotes $p < 0.01$ compared with shSCR.

hDna2 nuclease and/or helicase activities contribute to genomic stability in mammalian cells. To assess the roles of these activities, we carried out a series of genetic knockdown-rescue experiments utilizing an shRNA targeting the 3′-untranslated region (UTR) of endogenous hDna2 while expressing a FLAG-tagged shRNA-resistant hDna2 cDNA. We expressed either a control vector (ctrl) or wild-type (wt) hDna2, nuclease-deficient D294A (nuc) hDna2, or helicase/ATPase-deficient K671E (hel) hDna2 cDNA (5). To distinguish between the endogenous and exogenous hDna2 mRNAs, we designed specific PCR primers that amplify a region encompassing the last exon (exon 21) and the 3′-UTR of the endogenous hDna2 gene that is absent in the cDNA constructs. This allowed us to

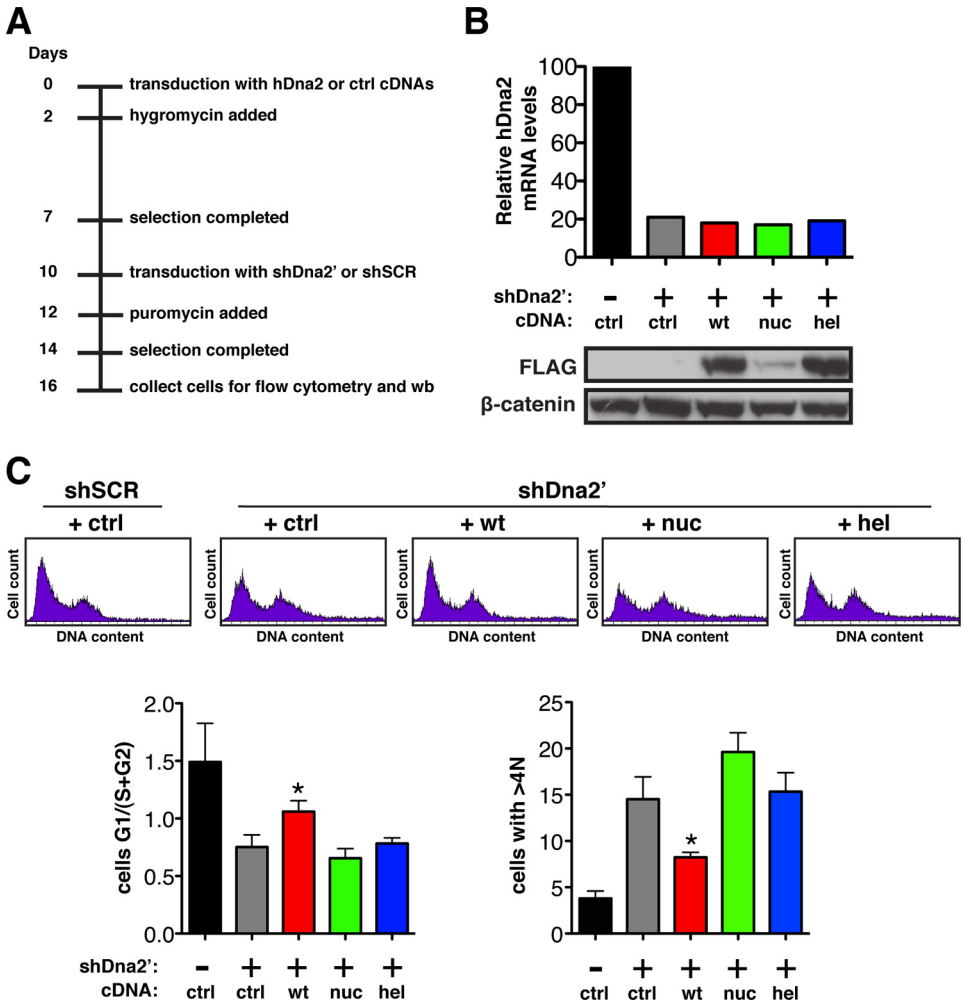

FIGURE 2. **hDna2 nuclease and helicase activities contribute to genomic stability.** *A*, shown is a timeline of the experimental procedures given in days; *wb* denotes Western blot. *B*, relative knockdown of hDna2 in U-2-OS cells was determined by quantitative RT-PCR (*top panel*). Results are normalized to cells co-expressing the control vector (*ctrl*) + shSCR (−). PCR primers used detect only endogenous hDna2 mRNA. cDNA construct expression was confirmed by anti-FLAG Western blot. *C*, flow cytometric analysis depicts the cell cycle and DNA content of the U-2-OS cells analyzed in *B*. *bar graphs* represent four independent experiments. *Left*, shown is the ratio of the percent of cells in G_1 *versus* the percent of cells in $S + G_2$. *Right*, shown is the percent of aneuploid cells containing abnormally high DNA content (>4N). *Error bars* represent S.E. for four independent experiments, and * denotes $p < 0.05$ compared with cells co-expressing the control vector + shDna2′.

confirm the knockdown of endogenous hDna2 while verifying ectopic expression of the cDNAs by Western blot using a FLAG antibody (Fig. 2, *A* and *B*).

We previously demonstrated that depletion of endogenous hDna2 results in a reduced G_1 population, a late S/G_2 cell cycle arrest, and the appearance of aneuploid cells (1). To assess the role of the helicase and nuclease activity of hDna2, we utilized flow cytometry to measure DNA content and determine the cell cycle profile of cells expressing wild-type or mutant hDna2. Expression of the wild-type allele significantly rescued the cell cycle defects observed upon depletion of hDna2 (Fig. 2*C*). In contrast, expression of the nuclease-deficient or helicase-deficient alleles did not rescue the cell cycle defects, indicating that both activities are essential to maintain genomic stability (Fig. 2*C*). Furthermore, cells expressing the nuclease-deficient hDna2 protein at even lower levels than the wild-type or helicase-deficient mutants displayed cell cycle defects that were more severe than those observed in cells depleted of endogenous hDna2 alone (Fig. 2, *B* and *C*, compare $G_1/(S + G_2)$ ratio, and cells with >4N DNA content). Interestingly, cells expressing high levels of the nuclease deficient allele were selected against over the course of the experiment as evidenced by a significant reduction in protein level, suggesting that the nuclease-deficient mutant is either toxic or functions as a dominant negative (Fig. 2, *A*–*C*).

To address whether hDna2 helicase activity contributed to the deleterious properties of the nuclease-deficient Dna2 allele, we expressed a double mutant (dm) allele lacking both the hDna2 nuclease and helicase activities. As seen in supplemental Fig. 2*B*, expression of the double mutant was maintained at levels similar to the helicase-deficient protein in contrast to the nuclease-deficient mutant whose expression was rapidly lost (supplemental Fig. 2, *A* and *B*). These results suggest that the toxic effect of nuclease-deficient hDna2 depends on its helicase activity and that both activities are coupled *in vivo*. Together, these results demonstrate that the nuclease and helicase activities of hDna2 are essential to maintain genomic stability.

hDna2 Interacts with Replisome Protein And-1 in a Replication-dependent Manner—Above, we demonstrate that hDna2 depletion leads to DNA damage and the appearance of meta-

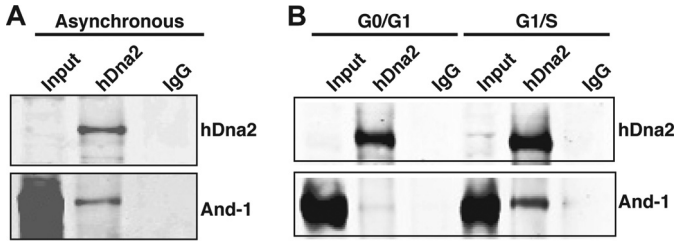

FIGURE 3. **hDna2 interacts with And-1 in a replication-dependent manner.** *A*, shown is the interaction between hDna2 and And-1 in asynchronous cells. hDna2 was immunoprecipitated from asynchronous HeLa cells followed by Western blot analysis with antibodies against And-1 or hDna2 as indicated. *B*, interaction between hDna2 and And-1 occurs during G_1/S transition. HeLa cells were arrested in G_0/G_1 by serum starvation or during G_1/S by a double thymidine block. hDna2 was immunoprecipitated from the arrested cells, and Western blot analysis was performed with antibodies against And-1 or hDna2 as indicated.

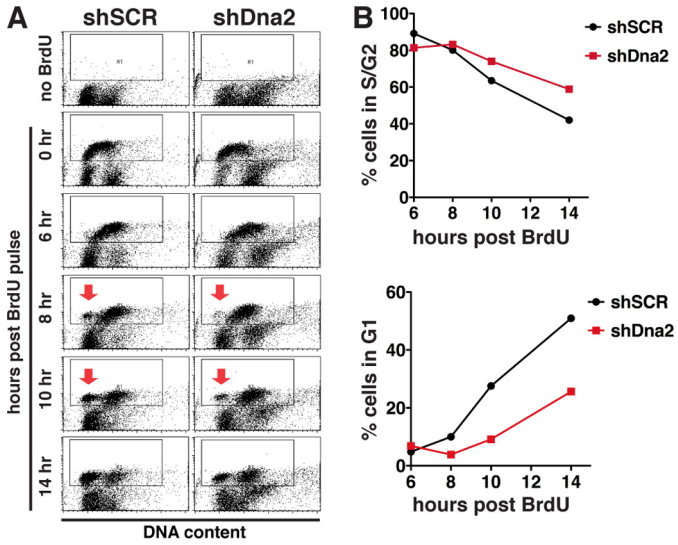

FIGURE 4. **hDna2 depletion impedes cell cycle progression in late S/G_2.** *A*, cell cycle progression is shown. U-2-OS cells expressing shSCR or shDna2 were pulsed with BrdU for 30 min and analyzed at the indicated times by flow cytometry using an anti-BrdU antibody (FITC-conjugated) (*y* axis) and propidium iodide to quantify DNA content (*x* axis). The *inset box* represents BrdU-positive cells that are analyzed in *B*. *Red arrows* indicate the cells appearing back in G_1 8 and 10 h post-BrdU pulse. *B*, shown is quantification of BrdU-positive cells in S/G_2 phase (*top graph*) or BrdU-positive cells appearing in G_1 (*bottom graph*). A representative experiment is shown.

phases reminiscent of cells entering mitosis with incomplete DNA replication. In *Xenopus laevis* extract, Dna2 is recruited to DNA shortly after replication licensing where it interacts with the replisome protein And-1 (47). To determine whether Dna2 associates with the replisome in human cells, we investigated interactions between hDna2 and And-1. We found that endogenous And-1 co-immunoprecipitated with hDna2 from asynchronous cells, suggesting that hDna2 associates with the replisome (Fig. 3*A* and data not shown). Furthermore, comparisons of the And-1/hDna2 interaction in cells arrested in G_0/G_1 by serum starvation and cells blocked at the G_1/S border by a double thymidine treatment revealed a significant increase in And-1/hDna2 interaction in cells arrested at the G_1/S transition (Fig. 3*B*). These observations demonstrate that hDna2 specifically interacts with And-1 in replicating cells and are similar to observations made in *Xenopus* extract (47). Together they suggest that hDna2 interacts with And-1 shortly after licensing of the pre-replication complex as part of the replisome.

hDna2 Depletion Leads to Replication Checkpoint Activation—Dna2 plays an essential role in DNA replication in yeast. Our results indicate a corresponding, important role in human DNA replication. Therefore, we next tested whether hDna2 depletion altered S phase progression. Control or hDna2-depleted U-2-OS cells were pulsed with BrdU for 30 min and chased for 12 h. Although hDna2-depleted cells incorporated BrdU at the same rate as control cells, they displayed a marked delay in completing the S/G_2 phase and consequently took longer to appear in the next G_1 phase after mitosis (Fig. 4, *A* and *B*) (compare 8-, 10-, and 12-h time points). These observations support the original cell cycle profiling data and suggest that hDna2 depletion alters late S/G_2 replication rather than bulk DNA replication rates during S phase. Furthermore, Western blot analysis revealed a reduction in the phosphorylation of the mitotic marker histone H3 at serine 10 in depleted *versus* control cells, confirming that the block occurs before mitosis (Fig. 5*A*, *bottom panel*).

Complete replication of the genome relies on efficient replication initiation, progression, and maturation. When replication is inhibited at any of these steps, cells respond by activating the S-phase checkpoint. Therefore, given the characteristic damage and cell cycle arrest observed after hDna2 depletion, we next investigated the activation status of Chk1. Western blot analysis of hDna2-depleted cells revealed a significant increase in phosphorylation of Chk1 at serine 317 compared with control cells, indicative of DNA replication stress (Fig. 5*A*, *top panel*). In agreement with this finding, we observed an accumulation of single-stranded DNA, a trigger of the S-phase checkpoint, as evidenced by a significant increase in the number of RPA foci per cell in hDna2-depleted cells compared with control cells (Fig. 5*B*).

Chk1 activation prevents cells that have not completed DNA replication from moving into mitosis (48). When Chk1 is inhibited in cells undergoing replication stress, they can move into mitosis with incompletely replicated DNA that if unrepaired will lead to unresolved replication intermediates. To address whether checkpoint activation blocked hDna2-depleted cells from entering mitosis with under-replicated chromosomes and/or unresolved damage, we treated cells with one of two Chk1 inhibitors, Gö 6976 or AZD7762 (38, 39). Cells depleted of hDna2 were grown for 8 h in the presence of the Chk1 inhibitor. Flow cytometric analysis revealed a drastic alteration in the cell cycle profile of hDna2-depleted cells treated with a Chk1 inhibitor compared with untreated cells (Fig. 5*C*). hDna2-depleted cells treated with the Chk1 inhibitor and released from the G_2 arrest entered mitosis but displayed an increase in ICBs compared with untreated hDna2-depleted cells, indicating that cells released from the G_2 block underwent aberrant mitosis (Fig. 5*D*). Together these experiments establish that cells depleted of hDna2 display replication defects and arrest in late S/G_2 due to checkpoint activation. Upon checkpoint override, cells resume cell cycle progression despite incomplete replication and/or unresolved damage and undergo aberrant mitoses.

Above we demonstrate that hDna2 depletion leads to Chk1 activation and a late S/G_2 cell cycle arrest. Chk1 activation after replicative stress occurs to stabilize ongoing replication forks

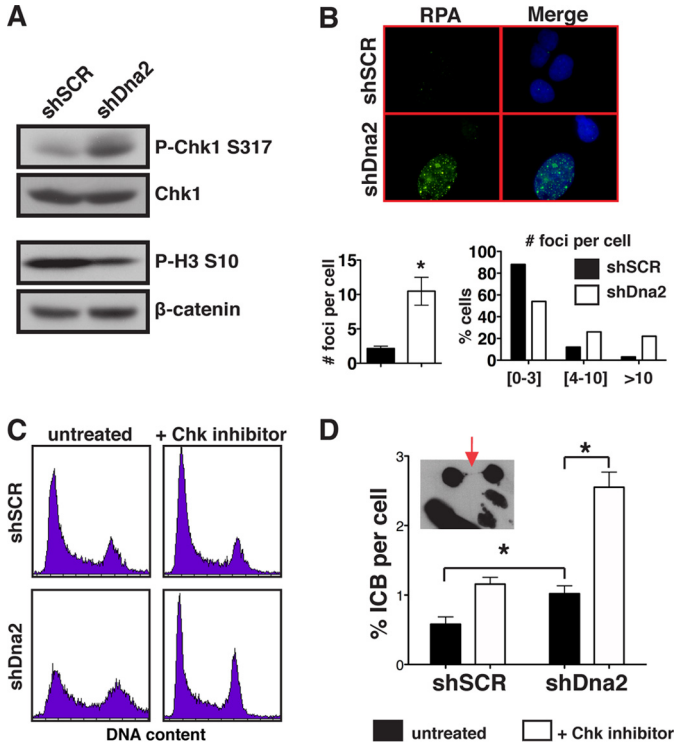

FIGURE 5. **hDna2 depletion activates the replication checkpoint.** *A*, Western blot analysis of control (*shSCR*) and hDna2-depleted (*shDna2*) U-2-OS cells is shown. Whole cell lysates were probed for total *versus* phosphorylated-Chk1 (*P-Chk1 S317*) (*top panels*). Samples were also probed for phosphorylated-histone H3 (*P-H3 S10*). *B*, immunofluorescence staining of RPA-70 in shSCR and shDna2 U-2-OS cells is shown. Cells were pre-extracted before fixing and staining to eliminate cytoplasmic RPA-70 (37). Quantification of RPA foci: average number (*left*) and total number (*right*) of foci per cell. * denotes $p < 0.01$. *C*, cell cycle distribution of shSCR and shDna2 +/− treatment with Chk1 inhibitor (Gö 6976) for 8 h. Similar results were obtained when AZD7762 was used to inhibit Chk1 (data not shown). *D*, ICBs (1) were quantified in control (*shSCR*) and hDna2-depleted (*shDna2*) U-2-OS cells ± Chk1 inhibitor. A representative image is shown with an ICB indicated by an *arrow*. * denotes $p < 0.01$.

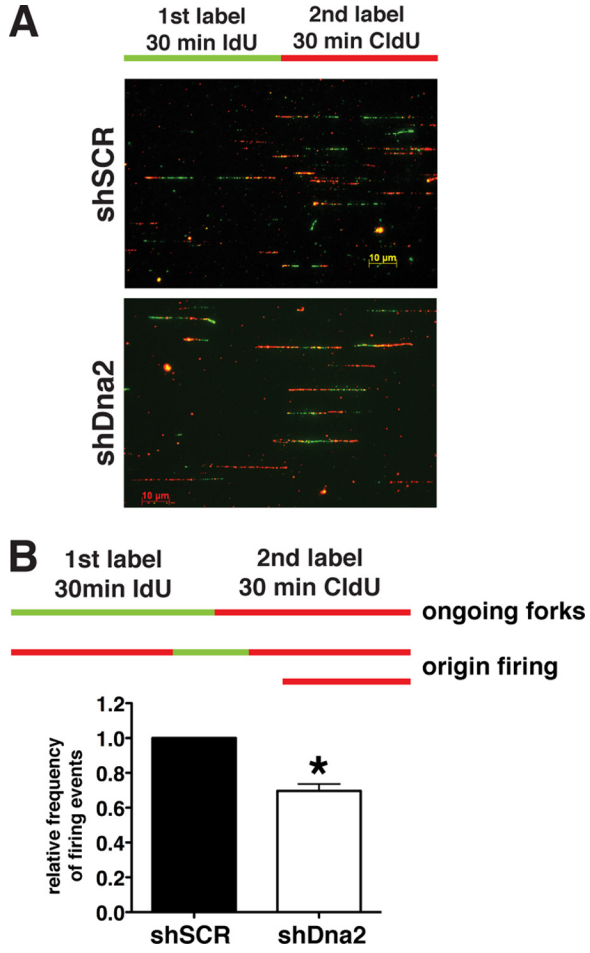

FIGURE 6. **hDna2 depletion reduces origin firing.** *A*, shSCR or shDna2 U-2-OS cells were labeled consecutively with IdU (*green*) and CldU (*red*) for 30 min each before isolating and stretching DNA for immunostaining. *B*, origin firing events among all tracks labeled were identified as CldU-only (*red only*) or CldU-IdU-CldU (*red-green-red*) triple-segment tracks. The mean percentages of new origin firing events defined by these two track types among all labeled tracks are shown for three independent experiments in which 200–450 tracks/experiment were analyzed for control shSCR or shDna2. *Error bars* show S.E. between three independent experiments. * denotes $p < 0.05$.

and to inhibit firing of additional forks (48). Therefore, to examine the impact of Chk1 activation on origin firing we used maRTA, wherein DNA is sequentially labeled *in vivo* with short pulses of the base analogues IdU and CldU (42). After labeling, DNA is isolated and stretched on coverslips for detection by IdU and CIdU immunostaining (Fig. 6*A*). Using maRTA, we quantified the fraction of DNA origin firing events present among all tracks labeled with CldU and IdU. We found that hDna2-depleted cells displayed a 20–25% reduction in origin firing events compared with control cells (Fig. 6*B*). Together, these experiments establish that hDna2 depletion activates the replication checkpoint, which in turn inhibits the firing of replication forks.

Defects in Okazaki Fragment Processing Do Not Alter Replication Fork Progression—Given the type of DNA damage we observed after hDna2 depletion and the model established in yeast suggesting Dna2 participates in OF maturation (9, 10), we next examined the role of hDna2 in DNA replication and fork progression using maRTA. By measuring the lengths of first label segments within replication tracks containing both labels, we determined the rate of DNA replication elongation. Using this method, we found that hDna2 depletion did not alter replication fork rate. Indeed, we found that DNA track lengths were similar in control and hDna2-depleted cells (Fig. 7*A*). This finding suggests that the damage that arises from unprocessed DNA fragments accumulating behind the replication fork does not impede continued replication fork progression and is consistent with our result showing no defects in S phase progression in hDna2-depleted cells (Fig. 4, *A* and *B*).

To further address the possibility that unprocessed OFs do not impact replication kinetics, we also depleted cells of FEN1 (supplemental Fig. 3) (10). Because FEN1 is the major OF processing nuclease in the cell, we expected to find that FEN1 depletion would alter replication fork progression. Strikingly, we found that FEN1 depletion also failed to slow replication fork progression. In fact, we found that DNA track lengths were slightly longer in FEN1-depleted cells compared with control cells (Fig. 7*B* and supplemental Fig. 3). Together these observations strongly suggest that the presence of unprocessed OFs and the associated damage they generate behind the replication fork is not sufficient to slow replication fork progression *in vivo*.

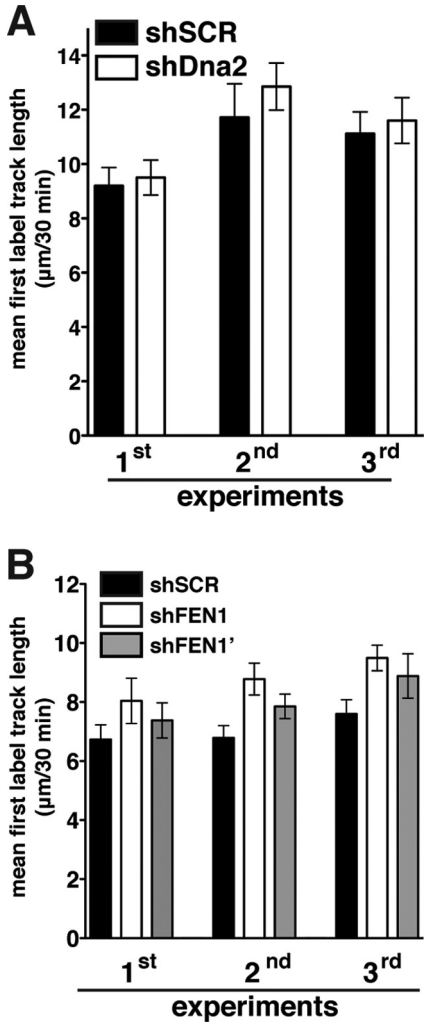

FIGURE 7. **Replication fork progression is unperturbed in hDna2- or FEN1-depleted cells.** *A*, quantification of three independent maRTA experiments is shown on the *right*. The *bar graph* summarizes mean lengths of first-label segments labeled for 30 min in two-segment tracks (*i.e.* tracks labeled consecutively with IdU and CIdU) to ensure that fork rate measurements were made from active replication forks. *Error bars* show 95% confidence intervals for sample means. No statistical difference in mean track lengths was observed between shSCR and shDna2 cells using a two-sample Kolmogorov-Smirnov test. *B*, shown are quantification of three independent experiments summarizing mean track length of the first label in cells depleted of FEN1 (*shFEN1*, *shFEN1'*) or control cells (shSCR).

hDna2 Depletion Does Not Lead to Detectable Defects in Maturation of Newly Synthesized DNA—Long flaps requiring Dna2 for processing are predicted to arise in only a small percentage of OFs, and in specific regions of the genome (4, 12, 20). Therefore, the need for Dna2 should be dispensable for processing the vast majority of OFs, in contrast to the short flaps that are cleaved by FEN1. To determine whether hDna2 participates in OF processing, we measured the maturation kinetics of newly replicated DNA using a BrdU-comet assay. We reasoned that if hDna2 were necessary to process only a minority of the flaps, it would be difficult to observe maturation differences in cells depleted of hDna2 alone. Therefore, we also depleted FEN1 in addition to hDna2 in an effort to increase the accumulation of long flaps that would require Dna2 activity. In parallel, we also depleted cells of DNA ligase I (LigI) as a positive control; LigI is required to ligate OF, which is required to complete OF processing (41). Western blot analysis demonstrated that we successfully depleted FEN1, LigI, or hDna2 alone and co-depleted FEN1 and hDna2 (Fig. 8*A*).

To assess the maturation of newly replicated DNA, control cells and cells depleted of hDna2, FEN1, or LigI alone or co-depleted of both hDna2 and FEN1 were pulsed with BrdU and analyzed by an alkaline comet assay. Immunofluorescence against BrdU was used to assess the integrity of newly replicated DNA by measuring its migration from the tail (unligated DNA fragments, *i.e.* unprocessed OFs) to the head (ligated DNA, *i.e.* processed OFs) of the comet (Fig. 8*B* compare 1-h to 8-h images). As expected, LigI depletion slowed the maturation of newly replicated DNA from comet tails to heads (Fig. 8*C*) (41). In contrast, we failed to observe a significant difference in OF maturation in hDna2-depleted compared with control cells (Fig. 8*C*). Furthermore, FEN1-depleted cells displayed a reduction similar to that of LigI-depleted cells, indicating that FEN1 is the major flap endonuclease responsible for processing OFs during lagging strand replication. Finally, OF maturation did not differ in FEN1-hDna2 co-depleted cells compared with cells depleted of FEN1 alone (Fig. 8*C*), suggesting that hDna2 does not compensate for FEN1 loss in OF processing. These results indicate that the DNA damage that arises upon hDna2 depletion (Fig. 9*C*, compare shDna2 to shFEN1 γ-H2AX levels) is unlikely to arise from a global OF maturation defect. However, it does not rule out a role for hDna2 in the maturation of a small fraction of OFs.

To further assess whether hDna2 primary function in DNA replication involves OF processing, we ectopically expressed FEN1 in hDna2-depleted cells (Ref. 33 and data not shown). In yeast, FEN1 overexpression compensates for phenotypes caused by hypomorphic mutations of Dna2 (8). However, ectopic expression of FEN1 in human cells did not improve the cell cycle defects observed in hDna2-depleted cells (Fig. 9, *A* and *B*). These results further reinforce the contention that the key role of hDna2 in DNA replication is independent of FEN1 or OF processing.

DISCUSSION

In this study we provide evidence that hDna2 is essential to ensure faithful replication of the genome like its yeast homologue and that unlike in yeast this essential role is independent of a requirement for hDna2 in global OF processing. We further demonstrate that both the nuclease and helicase activities of hDna2 contribute to genomic stability in human cells as they do in yeast. Finally, we report the unexpected finding that defective OF processing has no detectable impact on replication fork progression. This surprising result indicates that fork movement is decoupled from damage that arises behind the replication fork.

In *S. cerevisiae*, temperature-sensitive *dna2* mutant alleles arrest cells in G_2 with a 2C DNA content when shifted to the restrictive temperature (49). In *Schizosaccharomyces pombe,* temperature-sensitive mutants also arrest in late S phase but display no defects in bulk DNA synthesis (4). When combined with a checkpoint inhibitor, these cells bypass the arrest and undergo aberrant mitosis. Similarly, here we demonstrate that hDna2-depleted cells harbor DNA damage and arrest in late

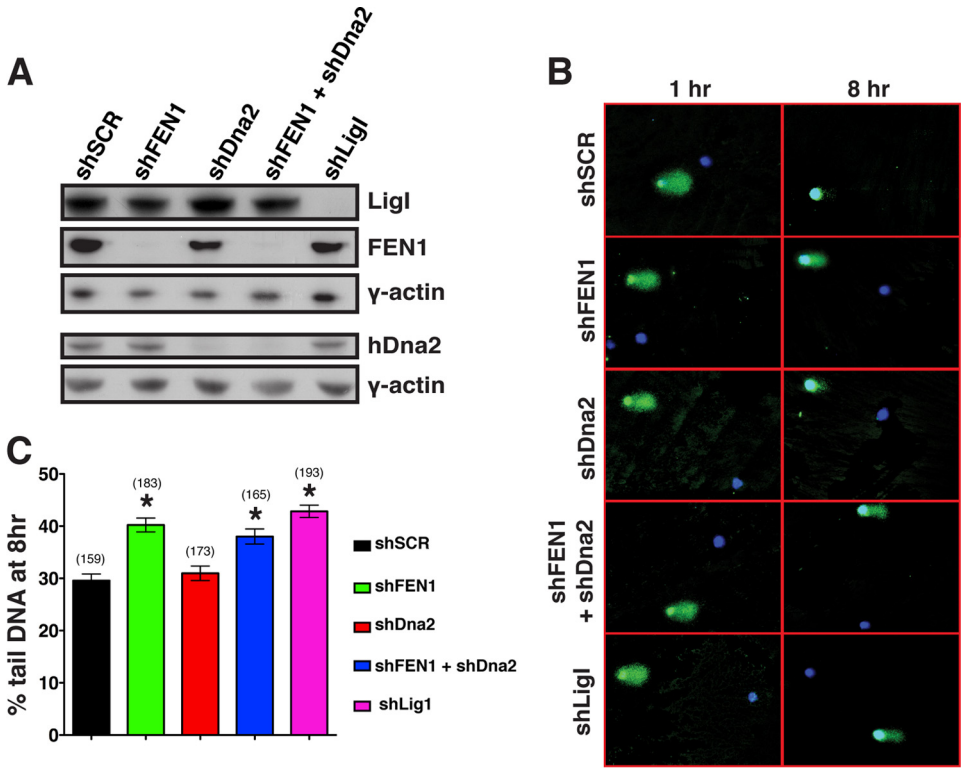

FIGURE 8. **hDna2 depletion does not impact Okazaki fragment maturation.** BrdU-comet analysis of U-2-OS cells depleted of FEN1 (*shFEN1*), hDna2 (*shDna2*), LigI (*shLigI*), or co-depleted of FEN1 and hDna2 (*shFEN1* + *shDna2*). Cells were pulsed for 15 min with BrdU and chased for 1 or 8 h before comet processing. *A*, shown is Western blot analysis of the different cell lines probed for LigI, FEN1, and hDna2. *B*, representative images of the different samples at 1 and 8 h post-BrdU pulse are shown. Cells were immunostained for BrdU (*green*), and DNA was stained with DAPI (*blue*). *C*, shown is quantification of the percent BrdU-positive DNA in the tail *versus* the comet head at the 8-h time point. Results are based on the analysis of 40–65 comets per experiment. A total of three independent experiments were performed, and the *errors bars* correspond to the S.E. The total number of cells analyzed per sample is shown in *parenthesis*. * denotes $p < 0.05$ comparing shFEN1, shFEN1+shDna2, or shLigI to shSCR.

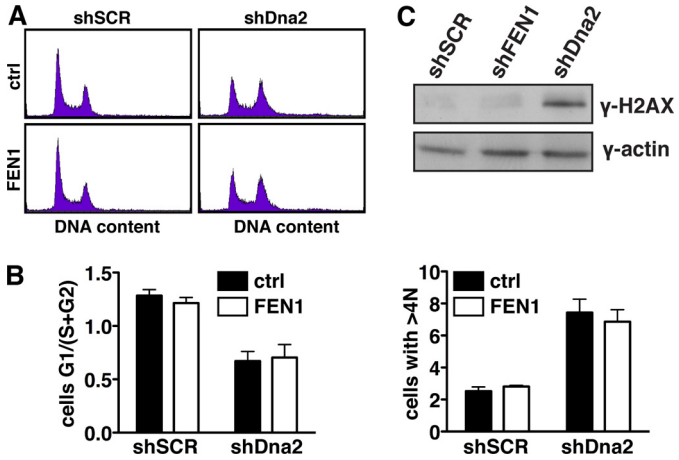

FIGURE 9. **FEN1 overexpression does not compensate for hDna2 depletion.** *A*, hDna2-depleted (*shDna2*) or control U-2-OS cells (*shSCR*) were transduced with either GFP (*ctrl*) or FLAG-FEN1 (*FEN1*). Immunofluorescence images against FLAG demonstrated >70% of transduction of FEN1 expressing cells (data not shown). Flow cytometry histograms of the cell cycle distribution of the respective cell lines are depicted with the cell count represented on the *y* axis and DNA content on the *x* axis. *B*, quantification of two independent experiments is shown. *Left*, shown is a graph representing the ratio of the percent of cells in G_1 *versus* the percent of cells in $S+G_2$. *Right*, shown is a graph representing the percent of cells containing abnormally high DNA content (>4N). *Error bars* represent S.E. C. γ-H2AX levels were determined by Western blot analysis in FEN1- or hDna2-depleted cells.

S/G_2 phase. Upon Chk1 inhibition, cells bypass the replication checkpoint and progress through mitosis, displaying aberrant mitotic structures (increase in ICBs; Fig. 5*D*). These phenotypes recapitulate observations in yeast and strongly suggest a conserved role for Dna2 in DNA replication in humans. Supporting our conclusions, ectopic expression of hDna2 suppresses the growth defects of the replication mutant *dna2–1* in *S. cerevisiae* (50).

The requirement for Dna2 helicase activity for yeast viability in *S. cerevisiae* indicates that this function is required *in vivo* (46). Indeed, different studies have demonstrated that Dna2 helicase activity is essential for efficient cleavage of long DNA flaps that may form secondary structures (7, 51). However, several studies demonstrated that the helicase activity of hDna2 is weak or undetectable and might not serve a corresponding role in human cells (5, 6). Our observation that neither nuclease nor helicase-deficient hDna2 mutants rescue hDna2 depletion demonstrates that both activities are essential to ensure the integrity of the genome. Furthermore, we provide evidence that as in yeast, hDna2 nuclease-deficient expression is toxic to the cell (46, 51). This toxicity depends on its helicase activity, suggesting that both activities need to be coupled within a single Dna2 molecule to act on its substrates *in vivo*. This is in contrast to Dna2 function in 5′ end resection during DSB repair where only the nuclease activity of Dna2 participates in this process (24, 28, 29, 53).

OF processing is an essential process that ensures a continuous lagging DNA strand and avoids single and double strand break formation. Several prior studies have suggested that defects in OF processing do not impact the rate of DNA syn-

thesis. Indeed, we previously demonstrated that FEN1 depletion did not slow S-phase progression or SV40 LargeT antigen-dependent DNA replication *in vitro* (33). Similarly, LigI mutant cells (46BR.1G1) that exhibit low LigI activity do not activate the intra-S phase checkpoint (41). Although protein extracts from these cells are deficient in OF ligation during SV40 DNA replication *in vitro*, they support incorporation of [α-^{32}P] dATP into plasmid DNA with similar kinetics as extracts from control fibroblasts (56). In addition, yeast deficient in LigI completely replicate their genomes despite being unable to ligate OF (54, 55). Together these studies suggest that replication fork progression is unperturbed in the absence of LigI. Here, using the sensitive maRTA technique, we demonstrate that depletion of an essential OF maturation protein, FEN1, does not alter replication fork progression *in vivo*. These observations strongly suggest that flaps that persist behind the replication fork do not affect the synthesis rate of DNA during replication.

FEN1 is postulated to be the primary endonuclease that processes flaps produced during lagging strand synthesis. However, both genetic and biochemical data indicate the presence of an additional long-flap processing pathway. Long DNA flap formation is promoted by PIF1 *in vitro* and requires Dna2 activity to create shorter flaps that are cleaved by FEN1 to generate a ligatable nick (9, 10, 14). To address the role of hDna2 in long-flap processing in human cells, we depleted FEN1 and hDna2 independently or together and then measured the maturation of nascent DNA. We found that maturation occurs with slower kinetics in FEN1-depleted cells, thus confirming FEN1 as the primary endonuclease responsible for processing OFs in human cells. In contrast, we did not observe a defect in maturation in hDna2-depleted cells. This indicates that if hDna2 processes long flaps, it does not represent a significant fraction of OFs in accordance with the model. However, our finding that FEN1-hDna2 co-depletion did not result in a significant difference in OF maturation rate compared with cells depleted of FEN1 alone was surprising, as in yeast *dna2* and *rad27*, mutations are synergistic (8). These results suggest either long flaps do not form readily in the absence of FEN1 in human cells or that another nuclease can process flaps to render them ligatable. In yeast, other nucleases such as RNaseH2 or Exo1 can compensate for FEN1 loss by processing short flaps (20, 57–59). It remains to be seen whether their functions are conserved in humans. Despite the apparent functional dominance of FEN1, we were surprised to find that hDna2-depleted cells display more DNA damage than FEN1-depleted cells as assessed by γ-H2AX levels and abnormal cell cycle profile (Fig. 9*B* and data not shown). One explanation for this is that even infrequent unprocessed long flaps are a source of DNA damage and genetic instability in the absence of hDna2. However, we find this to be unlikely because ectopic FEN1 expression had no impact on the defects observed in hDna2-depleted cells. Thus a more likely and interesting possibility is that hDna2 has an important, as yet to be elucidated, role in replication or DNA repair beyond its postulated role in OF processing. This possibility is strengthened by our observation that hDna2 interacts with And-1 specifically in replicating but not resting human cells. This interaction is in accordance with yeast and *Xenopus* observations (47, 52, 60, 61) and suggests that hDna2 is a component of the replication fork. The late S/G_2 phase arrest and appearance of aberrant post-mitotic structures could suggest a role for hDna2 in completing DNA replication by aiding in the resolution of replication intermediates. Interestingly, the Bloom RecQ helicase can resolve late replication intermediates, and its ectopic expression rescues Dna2 mutants in yeast (50). Alternatively, *Xenopus* Dna2 has been proposed to play a role in the early steps of DNA replication (3, 47). It remains to be addressed whether hDna2 actively participates in any of these processes.

Acknowledgments—We thank Dr. Soza and Dr. Montecucco for the BrdU-comet assay protocol and technical assistance with the procedure, Dr. Junran Zhang and Dr. Wei Shi for the RPA immunofluorescence protocol and aliquots of the antibody, Megan Ruhland, Avi Silver, and Keffy Kehrli for technical assistance, and members of the Stewart, Campbell, and Monnat laboratories for useful comments. We also thank Ermira Pazolli and Daniel Teasley for critical reading of the manuscript. We thank the The RNAi Consortium, Children's Discovery Institute and Washington University Genome Center for the RNAi constructs.

REFERENCES

1. Duxin, J. P., Dao, B., Martinsson, P., Rajala, N., Guittat, L., Campbell, J. L., Spelbrink, J. N., and Stewart, S. A. (2009) Human Dna2 is a nuclear and mitochondrial DNA maintenance protein. *Mol. Cell. Biol.* **29,** 4274–4282
2. Budd, M. E., and Campbell, J. L. (1995) A yeast gene required for DNA replication encodes a protein with homology to DNA helicases. *Proc. Natl. Acad. Sci. U.S.A.* **92,** 7642–7646
3. Liu, Q., Choe, W., and Campbell, J. L. (2000) Identification of the *Xenopus laevis* homolog of *Saccharomyces cerevisiae* DNA2 and its role in DNA replication. *J. Biol. Chem.* **275,** 1615–1624
4. Kang, H. Y., Choi, E., Bae, S. H., Lee, K. H., Gim, B. S., Kim, H. D., Park, C., MacNeill, S. A., and Seo, Y. S. (2000) Genetic analyses of *Schizosaccharomyces pombe* dna2(+) reveal that dna2 plays an essential role in Okazaki fragment metabolism. *Genetics* **155,** 1055–1067
5. Masuda-Sasa, T., Imamura, O., and Campbell, J. L. (2006) Biochemical analysis of human Dna2. *Nucleic Acids Res.* **34,** 1865–1875
6. Kim, J. H., Kim, H. D., Ryu, G. H., Kim, D. H., Hurwitz, J., and Seo, Y. S. (2006) Isolation of human Dna2 endonuclease and characterization of its enzymatic properties. *Nucleic Acids Res.* **34,** 1854–1864
7. Kang, Y. H., Lee, C. H., and Seo, Y. S. (2010) Dna2 on the road to Okazaki fragment processing and genome stability in eukaryotes. *Crit. Rev. Biochem. Mol. Biol.* **45,** 71–96
8. Budd, M. E., and Campbell, J. L. (1997) A yeast replicative helicase, Dna2 helicase, interacts with yeast FEN-1 nuclease in carrying out its essential function. *Mol. Cell. Biol.* **17,** 2136–2142
9. Bae, S. H., Bae, K. H., Kim, J. A., and Seo, Y. S. (2001) RPA governs endonuclease switching during processing of Okazaki fragments in eukaryotes. *Nature* **412,** 456–461
10. Ayyagari, R., Gomes, X. V., Gordenin, D. A., and Burgers, P. M. (2003) Okazaki fragment maturation in yeast. I. Distribution of functions between FEN1 AND DNA2. *J. Biol. Chem.* **278,** 1618–1625
11. Rossi, M. L., Purohit, V., Brandt, P. D., and Bambara, R. A. (2006) Lagging strand replication proteins in genome stability and DNA repair. *Chem. Rev.* **106,** 453–473
12. Rossi, M. L., Pike, J. E., Wang, W., Burgers, P. M., Campbell, J. L., and Bambara, R. A. (2008) Pif1 helicase directs eukaryotic Okazaki fragments toward the two-nuclease cleavage pathway for primer removal. *J. Biol. Chem.* **283,** 27483–27493
13. Kao, H. I., Veeraraghavan, J., Polaczek, P., Campbell, J. L., and Bambara, R. A. (2004) On the roles of *Saccharomyces cerevisiae* Dna2p and Flap endonuclease 1 in Okazaki fragment processing. *J. Biol. Chem.* **279,** 15014–15024
14. Bae, S. H., and Seo, Y. S. (2000) Characterization of the enzymatic prop-

erties of the yeast dna2 Helicase/endonuclease suggests a new model for Okazaki fragment processing. *J. Biol. Chem.* **275,** 38022–38031
15. Stewart, J. A., Campbell, J. L., and Bambara, R. A. (2006) Flap endonuclease disengages Dna2 helicase/nuclease from Okazaki fragment flaps. *J. Biol. Chem.* **281,** 38565–38572
16. Stewart, J. A., Miller, A. S., Campbell, J. L., and Bambara, R. A. (2008) Dynamic removal of replication protein A by Dna2 facilitates primer cleavage during Okazaki fragment processing in *Saccharomyces cerevisiae*. *J. Biol. Chem.* **283,** 31356–31365
17. Stewart, J. A., Campbell, J. L., and Bambara, R. A. (2009) Significance of the dissociation of Dna2 by flap endonuclease 1 to Okazaki fragment processing in *Saccharomyces cerevisiae*. *J. Biol. Chem.* **284,** 8283–8291
18. Stewart, J. A., Campbell, J. L., and Bambara, R. A. (2010) Dna2 is a structure-specific nuclease, with affinity for 5′-flap intermediates. *Nucleic Acids Res.* **38,** 920–930
19. Budd, M. E., Reis, C. C., Smith, S., Myung, K., and Campbell, J. L. (2006) Evidence suggesting that Pif1 helicase functions in DNA replication with the Dna2 helicase/nuclease and DNA polymerase δ. *Mol. Cell. Biol.* **26,** 2490–2500
20. Stith, C. M., Sterling, J., Resnick, M. A., Gordenin, D. A., and Burgers, P. M. (2008) Flexibility of eukaryotic Okazaki fragment maturation through regulated strand displacement synthesis. *J. Biol. Chem.* **283,** 34129–34140
21. Pike, J. E., Burgers, P. M., Campbell, J. L., and Bambara, R. A. (2009) Pif1 helicase lengthens some Okazaki fragment flaps necessitating Dna2 nuclease/helicase action in the two-nuclease processing pathway. *J. Biol. Chem.* **284,** 25170–25180
22. Pike, J. E., Henry, R. A., Burgers, P. M., Campbell, J. L., and Bambara, R. A. (2010) An alternative pathway for Okazaki fragment processing. Resolution of fold back-flaps by Pif1 helicase. *J. Biol. Chem.* **285,** 41712–41723
23. Choe, W., Budd, M., Imamura, O., Hoopes, L., and Campbell, J. L. (2002) Dynamic localization of an Okazaki fragment processing protein suggests a novel role in telomere replication. *Mol. Cell. Biol.* **22,** 4202–4217
24. Zhu, Z., Chung, W. H., Shim, E. Y., Lee, S. E., and Ira, G. (2008) Sgs1 helicase and two nucleases Dna2 and Exo1 resect DNA double-strand break ends. *Cell* **134,** 981–994
25. Liao, S., Toczylowski, T., and Yan, H. (2008) Identification of the *Xenopus* DNA2 protein as a major nuclease for the 5′→3′ strand-specific processing of DNA ends. *Nucleic Acids Res.* **36,** 6091–6100
26. Tomita, K., Kibe, T., Kang, H. Y., Seo, Y. S., Uritani, M., Ushimaru, T., and Ueno, M. (2004) Fission yeast Dna2 is required for generation of the telomeric single-strand overhang. *Mol. Cell. Biol.* **24,** 9557–9567
27. Bonetti, D., Martina, M., Clerici, M., Lucchini, G., and Longhese, M. P. (2009) Multiple pathways regulate 3′ overhang generation at *S. cerevisiae* telomeres. *Mol. Cell* **35,** 70–81
28. Niu, H., Chung, W. H., Zhu, Z., Kwon, Y., Zhao, W., Chi, P., Prakash, R., Seong, C., Liu, D., Lu, L., Ira, G., and Sung, P. (2010) Mechanism of the ATP-dependent DNA end-resection machinery from *Saccharomyces cerevisiae*. *Nature* **467,** 108–111
29. Cejka, P., Cannavo, E., Polaczek, P., Masuda-Sasa, T., Pokharel, S., Campbell, J. L., and Kowalczykowski, S. C. (2010) DNA end resection by Dna2-Sgs1-RPA and its stimulation by Top3-Rmi1 and Mre11-Rad50-Xrs2. *Nature* **467,** 112–116
30. Chen, X., Niu, H., Chung, W. H., Zhu, Z., Papusha, A., Shim, E. Y., Lee, S. E., Sung, P., and Ira, G. (2011) Cell cycle regulation of DNA double-strand break end resection by Cdk1-dependent Dna2 phosphorylation. *Nat. Struct. Mol. Biol.* **18,** 1015–1019
31. Nimonkar, A. V., Genschel, J., Kinoshita, E., Polaczek, P., Campbell, J. L., Wyman, C., Modrich, P., and Kowalczykowski, S. C. (2011) BLM-DNA2-RPA-MRN and EXO1-BLM-RPA-MRN constitute two DNA end resection machineries for human DNA break repair. *Genes Dev.* **25,** 350–362
32. Saharia, A., Guittat, L., Crocker, S., Lim, A., Steffen, M., Kulkarni, S., and Stewart, S. A. (2008) Flap endonuclease 1 contributes to telomere stability. *Curr. Biol.* **18,** 496–500
33. Saharia, A., Teasley, D. C., Duxin, J. P., Dao, B., Chiappinelli, K. B., and Stewart, S. A. (2010) FEN1 ensures telomere stability by facilitating replication fork re-initiation. *J. Biol. Chem.* **285,** 27057–27066
34. Zhu, W., Ukomadu, C., Jha, S., Senga, T., Dhar, S. K., Wohlschlegel, J. A., Nutt, L. K., Kornbluth, S., and Dutta, A. (2007) Mcm10 and And-1/CTF4 recruit DNA polymerase α to chromatin for initiation of DNA replication. *Genes Dev.* **21,** 2288–2299
35. Jackman, J., and O'Connor, P. M. (2001) Methods for synchronizing cells at specific stages of the cell cycle. *Curr. Protoc. Cell Biol.* Chapter 8, Unit 8.3
36. Diede, S. J., and Gottschling, D. E. (1999) Telomerase-mediated telomere addition *in vivo* requires DNA primase and DNA polymerases α and δ. *Cell* **99,** 723–733
37. Shi, W., Feng, Z., Zhang, J., Gonzalez-Suarez, I., Vanderwaal, R. P., Wu, X., Powell, S. N., Roti Roti, J. L., Gonzalo, S., and Zhang, J. (2010) The role of RPA2 phosphorylation in homologous recombination in response to replication arrest. *Carcinogenesis* **31,** 994–1002
38. Kohn, E. A., Yoo, C. J., and Eastman, A. (2003) The protein kinase C inhibitor Gö 6976 is a potent inhibitor of DNA damage-induced S and G_2 cell cycle checkpoints. *Cancer Res.* **63,** 31–35
39. Zabludoff, S. D., Deng, C., Grondine, M. R., Sheehy, A. M., Ashwell, S., Caleb, B. L., Green, S., Haye, H. R., Horn, C. L., Janetka, J. W., Liu, D., Mouchet, E., Ready, S., Rosenthal, J. L., Queva, C., Schwartz, G. K., Taylor, K. J., Tse, A. N., Walker, G. E., and White, A. M. (2008) AZD7762, a novel checkpoint kinase inhibitor, drives checkpoint abrogation, and potentiates DNA-targeted therapies. *Mol. Cancer Ther.* **7,** 2955–2966
40. Stewart, S. A., Poon, B., Jowett, J. B., and Chen, I. S. (1997) Human immunodeficiency virus type 1 Vpr induces apoptosis following cell cycle arrest. *J. Virol.* **71,** 5579–5592
41. Soza, S., Leva, V., Vago, R., Ferrari, G., Mazzini, G., Biamonti, G., and Montecucco, A. (2009) DNA ligase I deficiency leads to replication-dependent DNA damage and impacts cell morphology without blocking cell cycle progression. *Mol. Cell. Biol.* **29,** 2032–2041
42. Sidorova, J. M., Li, N., Schwartz, D. C., Folch, A., and Monnat, R. J., Jr. (2009) Microfluidic-assisted analysis of replicating DNA molecules. *Nat. Protoc.* **4,** 849–861
43. Saharia, A., and Stewart, S. A. (2009) FEN1 contributes to telomere stability in ALT-positive tumor cells. *Oncogene* **28,** 1162–1167
44. Mandahl, N., Mertens, F., Willén, H., Rydholm, A., Kreicbergs, A., and Mitelman, F. (1998) Nonrandom pattern of telomeric associations in atypical lipomatous tumors with ring and giant marker chromosomes. *Cancer Genet. Cytogenet.* **103,** 25–34
45. Nghiem, P., Park, P. K., Kim, Y., Vaziri, C., and Schreiber, S. L. (2001) ATR inhibition selectively sensitizes G_1 checkpoint-deficient cells to lethal premature chromatin condensation. *Proc. Natl. Acad. Sci. U.S.A.* **98,** 9092–9097
46. Budd, M. E., Choe, W., and Campbell, J. L. (2000) The nuclease activity of the yeast DNA2 protein, which is related to the RecB-like nucleases, is essential *in vivo*. *J. Biol. Chem.* **275,** 16518–16529
47. Wawrousek, K. E., Fortini, B. K., Polaczek, P., Chen, L., Liu, Q., Dunphy, W. G., and Campbell, J. L. (2010) *Xenopus* DNA2 is a helicase/nuclease that is found in complexes with replication proteins And-1/Ctf4 and Mcm10 and DSB response proteins Nbs1 and ATM. *Cell Cycle* **9,** 1156–1166
48. Cimprich, K. A., and Cortez, D. (2008) ATR: an essential regulator of genome integrity. *Nat. Rev. Mol. Cell Biol.* **9,** 616–627
49. Fiorentino, D. F., and Crabtree, G. R. (1997) Characterization of *Saccharomyces cerevisiae* dna2 mutants suggests a role for the helicase late in S phase. *Mol. Biol. Cell* **8,** 2519–2537
50. Imamura, O., and Campbell, J. L. (2003) The human Bloom syndrome gene suppresses the DNA replication and repair defects of yeast dna2 mutants. *Proc. Natl. Acad. Sci. U.S.A.* **100,** 8193–8198
51. Bae, S. H., Kim, D. W., Kim, J., Kim, J. H., Kim, D. H., Kim, H. D., Kang, H. Y., and Seo, Y. S. (2002) Coupling of DNA helicase and endonuclease activities of yeast Dna2 facilitates Okazaki fragment processing. *J. Biol. Chem.* **277,** 26632–26641
52. Araki, Y., Kawasaki, Y., Sasanuma, H., Tye, B. K., and Sugino, A. (2003) Budding yeast mcm10/dna43 mutant requires a novel repair pathway for viability. *Genes Cells* **8,** 465–480
53. Peng, G., Dai, H., Zhang, W., Hsieh, H. J., Pan, M. R., Park, Y. Y., Tsai, R. Y., Bedrosian, I., Lee, J. S., Ira, G., and Lin, S. Y. (2012) Human nuclease/helicase DNA2 alleviates replication stress by promoting DNA end resection. *Cancer Res.*, in press

54. Das-Bradoo, S., Nguyen, H. D., and Bielinsky, A. K. (2010) Damage-specific modification of PCNA. *Cell Cycle* **9,** 3674–3679
55. Das-Bradoo, S., Nguyen, H. D., Wood, J. L., Ricke, R. M., Haworth, J. C., and Bielinsky, A. K. (2010) Defects in DNA ligase I trigger PCNA ubiquitylation at Lys 107. *Nat. Cell Biol.* **12,** 74–79
56. Mackenney, V. J., Barnes, D. E., and Lindahl, T. (1997) Specific function of DNA ligase I in simian virus 40 DNA replication by human cell-free extracts is mediated by the amino-terminal non-catalytic domain. *J. Biol. Chem.* **272,** 11550–11556
57. Tishkoff, D. X., Boerger, A. L., Bertrand, P., Filosi, N., Gaida, G. M., Kane, M. F., and Kolodner, R. D. (1997) Identification and characterization of *Saccharomyces cerevisiae* EXO1, a gene encoding an exonuclease that interacts with MSH2. *Proc. Natl. Acad. Sci. U.S.A.* **94,** 7487–7492
58. Murante, R. S., Henricksen, L. A., and Bambara, R. A. (1998) Junction ribonuclease. An activity in Okazaki fragment processing. *Proc. Natl. Acad. Sci. U.S.A.* **95,** 2244–2249
59. Lee, B. I., and Wilson, D. M., 3rd. (1999) The RAD2 domain of human exonuclease 1 exhibits 5′ to 3′ exonuclease and flap structure-specific endonuclease activities. *J. Biol. Chem.* **274,** 37763–37769
60. Formosa, T., and Nittis, T. (1999) Dna2 mutants reveal interactions with Dna polymerase α and Ctf4, a Pol α accessory factor, and show that full Dna2 helicase activity is not essential for growth. *Genetics* **151,** 1459–1470
61. Budd, M. E., Tong, A. H., Polaczek, P., Peng, X., Boone, C., and Campbell, J. L. (2005) A network of multi-tasking proteins at the DNA replication fork preserves genome stability. *PLoS Genet* **1,** e61